PHYSICAL REVIEW A **69**, 051602(R) (2004)

Fluctuations and flux: The limits of multistate atom lasers

N. P. Robins,* C. M. Savage, J. J. Hope, J. E. Lye, C. S. Fletcher, S. A. Haine, and J. D. Close
Australian Centre for Quantum Atom Optics, The Australian National University, Canberra 0200, Australia
(Received 14 November 2003; published 19 May 2004)

By direct comparison between experiment and theory with no adjustable parameters, we show how the classical fluctuations on a multistate atom laser beam increase with increasing flux. The fluctuations are inherent to state changing out coupling, rf, Raman, or otherwise and are likely to be present in all atom lasers, pulsed or continuous, that employ such out coupling. If not removed or avoided, these classical fluctuations will prevent shot noise limited measurement employing atom lasers of this kind.

DOI: 10.1103/PhysRevA.69.051602 PACS number(s): 03.75.Pp, 03.75.Mn

It is the high flux, spectral density, and associated first order coherence that has made the optical laser central to many technologies. In the field of precision measurement, atom lasers hold similar promise [1]. In a Sagnac interferometer, for example, the inherent sensitivity of a matter wave gyroscope exceeds that of a photon gyroscope with the same particle flux and area by 11 orders of magnitude [2]. In the design of any precision interferometric experiment using a laser, the classical fluctuations of the source must be characterized and either avoided or removed in order to reach the quantum noise floor.

Although classical fluctuations are deterministic, they have real detrimental effects in precision measurements. There is a large literature for example characterizing the classical fluctuation spectrum in solid state optical lasers [3]. In these lasers, the spectrum of classical fluctuations is dominated by pump noise at low frequencies and the relaxation oscillation at higher frequencies. Characterization of the relaxation oscillation has allowed the implementation of devices such as "noise eaters," used in quantum optics labs around the world, to feedback to the laser, suppress classical fluctuations and achieve or surpass, through squeezing, the shot noise limit. Alternatively, many optical experiments are designed to avoid classical fluctuations of this kind either by moving the signal to a higher frequency band by modulation, and/or the use of an rf spectrum analyzer. Either way, the classical fluctuation spectrum must be well characterized for these approaches to succeed. Similarly, the characterization of classical fluctuations in atom lasers particularly those that are inherent to out coupling, is essential if they are to become a useful tool in precision measurement.

In this paper, we report the observation and study of classical fluctuations on an atom laser beam that are an unavoidable result of state changing out coupling. We find agreement between our experimental results and a full three-dimensional (3D) Gross-Pitaevskii (GP) model with no adjustable parameters, and show that at high flux, classical fluctuations increase with increasing flux. That we can achieve agreement between a 3D theory including all Zeeman states and experiment is significant. It is highly likely that the much sought-after pumped atom laser will operate under rather specific conditions of scattering length, temperature and number density [4], and experiments will need to be guided by accurate theoretical models that must be validated if we are to trust their detailed predictions.

Mewes *et al.* [5] demonstrated the first atom laser based on the application of pulsed radio-frequency (rf) fields to induce controlled spin flips from magnetically trapped to untrapped states of a Bose-Einstein condensate. Later it was shown by Hagley *et al.* that a pulsed Raman out coupling could be used to achieve a quasicontinuous multistate atomic beam [6]. Bloch *et al.* achieved continuous rf out coupling for up to 100 ms, producing a single state atom laser beam, and showed that this beam could be coherently manipulated in direct analogy to the optical laser [7,8]. Both temporal and spatial coherence have been measured, and it has been demonstrated that rf out coupling preserves the coherence of the condensate [9–11]. The beam divergence has been measured [12], and there has been one real time measurement of the flux of an atom laser beam [13]. Ballagh *et al.* [14] introduced the Gross-Pitaevskii equation as an effective tool for investigating the atom laser within the semiclassical mean-field approximation and a number of groups found good agreement between GP models and experiment [15,16]. Rabi cycling between Zeeman components, a manifestation of the non-Markovian nature of the atom laser [17,18], was observed in the experiment of Mewes *et al.* and could be expected to significantly increase the amplitude, and possibly frequency fluctuations of the beam. There has been no investigation of the relationship between classical fluctuations inherent to out coupling, and flux in an atom laser, and it is this aspect that we investigate both experimentally and theoretically in this paper.

Experimentally, a continuous atom laser based on resonant output coupling puts stringent limits on the stability of cold atom traps [7]. Typical condensates have a resonant width of 10 kHz. Output coupling requires a stable magnetic bias B_0 at the 0.1 mG level, one to two orders of magnitude better than typical magnetic traps. In comparison, a pulsed atom laser is relatively straightforward to implement. A 10 μs pulse has a frequency width of 200 kHz, significantly broader than both the 10 kHz resonant width of the condensate, and the instability of our trap which fluctuates within the range ±15 kHz due mainly to thermal fluctuations of the coils. In the work reported in this paper, we have opted to study a pulsed atom laser to ensure shot to shot reproducibility and allow detailed quantitative comparison to numerical

*Electronic address: nick.robins@anu.edu.au;
URL: http://www.acqao.org/

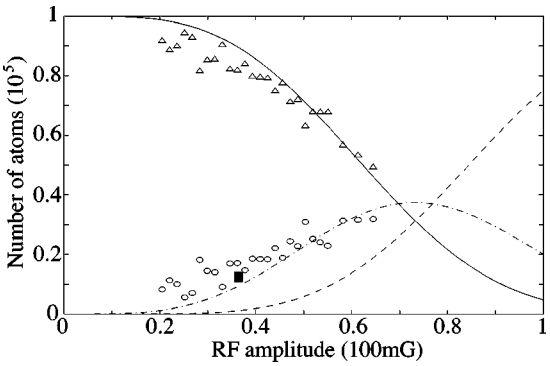

FIG. 1. Out-coupled fraction as a function of rf amplitude. The solid square is the power at which the results of Fig. 2 were generated. Theoretical curves are: Solid line, $m_F=2,1$ trapped states, dot-dashed $m_F=0$ and dashed, $m_F=-2,-1$ antitrapped states. The experimental results are: triangles, $m_F=2,1$ trapped states, circles $m_F=0$. Typical error bars are ±5% vertically and ±10% horizontally. Simulation parameter: $\Delta=-640$.

models. We have chosen to study atom laser beams derived from an $F=2, m_F=2$ condensate because of the richness and complexity offered by the system. The classical fluctuations we study, however, are likely to be present in all atom lasers, pulsed and continuous, that use any form of state changing out coupling, rf, Raman, or otherwise. We elaborate on this point in the conclusion. The recently published "all-optical" atom laser, where atoms spill over the top of an optical potential, offers an interesting alternative to state changing out coupling from a magnetic trap [19].

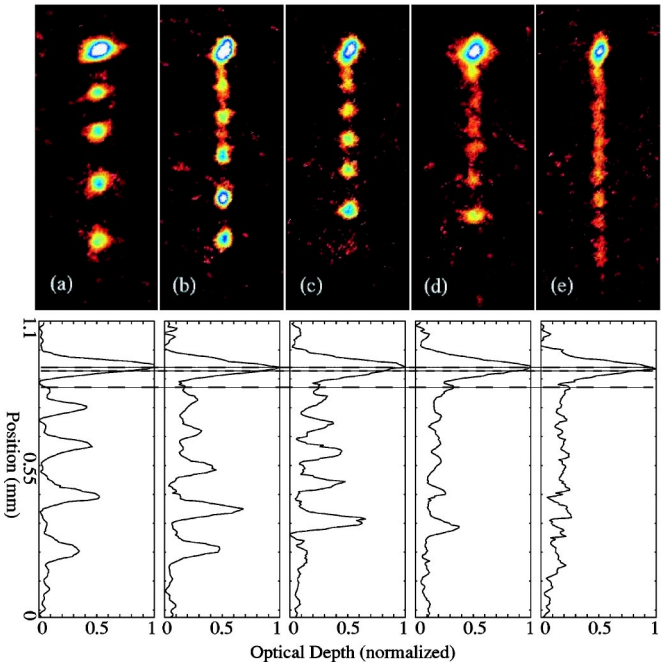

FIG. 2. (Color online) A series of pulsed atom lasers at different pulse rates. The applied radio-frequency (rf) pulses are varied from (a) four pulses, (b) five pulses, (c) six pulses, (d) seven pulses, (e) ten pulses in an 8 ms window. The lower plots show a cross-section down the center of the absorption data. The three dashed lines correspond in descending order to the center of the condensate, the half-width of the 200 kHz rf resonance (100 kHz ≈12 μm in our trap), and the position coinciding with the final rf out-coupling pulse (4 ms prior to imaging).

In our experiment, we produce an $F=2, m_F=2$ ^{87}Rb condensate, consisting of approximately 50 000 atoms, via evaporation in a water-cooled QUIC magnetic trap [20] with a radial trapping frequency $\nu_r=253$ Hz, an axial trapping frequency $\nu_z=20$ Hz, and a bias field $B_0=1$ G. After evaporative cooling, the BEC was left to equilibriate for 100 ms. We then triggered an rf signal generator set in gated burst mode. The rf pulses were amplified (35 dB) and radiated perpendicular to the magnetic bias field of the trap through a 22 mm radius single loop, approximately 18 mm from the BEC. To ensure that we had calibrated all experimental parameters correctly, we made an initial series of measurements of the number of trapped and untrapped atoms after the application of single rf pulses of varying amplitude; it was critical to establish agreement between experiment and theory in a simple mode of operation before pursuing studies of more complex dynamics. In Fig. 1, we show the results of these measurements in comparison with a one-dimensional Gross-Pitaevskii theory of the atom laser derived from the full 3D model described by the following equations:

$$
\begin{aligned}
i\dot{\phi}_2 &= (\mathcal{L} + V_T + Gy - 2\Delta)\phi_2 + 2\Omega\phi_1,\\
i\dot{\phi}_1 &= (\mathcal{L} + \tfrac{1}{2}V_T + Gy - \Delta)\phi_1 + 2\Omega\phi_2 + \sqrt{6}\Omega\phi_0,\\
i\dot{\phi}_0 &= (\mathcal{L} + Gy)\phi_0 + \sqrt{6}\Omega\phi_1 + \sqrt{6}\Omega\phi_{-1},\\
i\dot{\phi}_{-1} &= (\mathcal{L} - \tfrac{1}{2}V_T + Gy + \Delta)\phi_{-1} + 2\Omega\phi_{-2} + \sqrt{6}\Omega\phi_0,\\
i\dot{\phi}_{-2} &= (\mathcal{L} - V_T + Gy + 2\Delta)\phi_{-2} + 2\Omega\phi_{-1},
\end{aligned}
\qquad (1)
$$

where ϕ_i is the GP function for the ith Zeeman state. $V_T=\lambda^2(x^2+y^2)+z^2$, $\mathcal{L}\equiv -1/2\nabla^2+U(\Sigma_{i=-2}^{2}|\phi_i|^2)$. Here $\lambda=\nu_r/\nu_z=12.65$ is the ratio of trapping frequencies, Δ and Ω are respectively the detuning of the rf field from resonance and the Rabi frequency, measured in units of $\omega_z=2\pi\nu_z$. U is the two-body interaction coefficient and $G=z_0 mg/(\hbar\omega_z)$, where m is the atomic mass and g the acceleration due to gravity. $z_0=\sqrt{\hbar/m\omega_z}$ is the usual harmonic oscillator length. The wave functions, time, spatial coordinates, and interaction strengths are measured in the units of z_0 and ω_z^{-1}. The excellent agreement between experiment and theory shown in Fig. 1 indicates that we have a well calibrated and repeatable experiment. Up to the experimental uncertainty in the detuning Δ, there are no free parameters in the 1D GP model. The theoretical results of the Rabi oscillations presented in Fig. 1 are in good agreement with the approximate analytic theory presented by Graham and Walls for the limit of strong out coupling [21].

In the experimental data shown in Fig. 2, we present five pulse trains outcoupled from separate $F=2$, $m_F=2$ condensates. In each case, the pulse train has been outcoupled in an 8 ms time frame. We wait 2 ms after the pulse window before turning the trap off to allow the final atomic pulse to completely separate from the condensate. After a further 2 ms, to allow expansion of the condensate, we image the condensate and pulses with a single lens onto a 12 bit CCD camera. For one, two, three and four rf pulses, we observe

predictable out coupling from the atom laser system. Figure 2(a) is indicative of this behavior, where four rf pulses (separation 2 ms) have been applied to the BEC, and we see four $m_F=0$ atomic pulses in the positions expected from gravity. In Fig. 2(b) five rf pulses (separation 1.6 ms) have been applied and we observe five atomic wave packets, again in the expected positions. However, we note that in the latter three pulses there is a significant blurring with atoms appearing between the expected positions of the pulses. This effect is not due to interference between the wave packets.

The transition from constant pulse amplitude shown in Fig. 2(a) to varying or fluctuating pulse amplitude with increasing repetition rate shows a clear trade off between classical fluctuations and flux in the atom laser output. In Fig. 2(c) six rf pulses were applied (separation 1.2 ms), however, only five atomic pulses were observed, with the first atomic pulse being entirely absent. This observation is quite repeatable. The complete absence of a pulse is an extreme example of the trade off between classical fluctuations and flux, and it is the dynamics behind this phenomenon that we wished to understand by comparison with a complete 3D GP model. At the higher pulse repetition rate used in Fig. 2(d) where the separation between pulses is 1 ms, the output is further distorted from the ideal. In Fig. 2(e), where the time between pulses has been reduced to 800 μs, the atom laser beam is longer than expected from pure gravitational acceleration. This can be explained by the influence of the the antitrapped m_F states on the $m_F=0$ atoms that comprise the outcoupled beam. It is quite clear from the data that increasing flux (and therefore decreasing shot noise) comes at the price of increasing classical fluctuations.

We have quantitatively modeled the experiment with a full 3D GP simulation including all five Zeeman states and with no adjustable parameters [Eq. (1)]. This is a unique feature of the work presented here and allows us to understand all aspects of the GP physics, and hence the experiment. A 1D model accurately describes a single out-coupling pulse because it is essentially independent of the spatial structure. However, we found that a full 3D simulation was needed to accurately track the spatiotemporal dynamics of a multipulse experiment. We simulated up to 3.2 ms, allowing three pulses for each case. Parallelized code was run on twelve processors of the APAC National Facility [22], requiring up to 800 h of processor time per simulation. The numerical method was the psuedospectral method with Runge-Kutta split time step developed at the University of Otago [23]. Spatial grid sizes and time steps were monitored throughout the simulations to ensure the accuracy of the numerical solutions; e.g., the preservation of the normalization. Spatial grids were grown, and time steps decreased, as required. At the end of simulations, spatial grids in the direction of gravity were 2048 points for the trapped ($m_F=2,1$) and antitrapped ($m_F=-2,-1$) Zeeman states, and 4096 for the atom laser output state ($m_F=0$). In the tight and loose transverse directions, 128 and 32 points were used, respectively. The corresponding spatial lengths were chosen so that both the momentum space and real space GP functions fit the grid. This was about 40 and 140 μm in the tight and loose trap directions, respectively. In the direction of gravity, it was 120 μm for the $m_F\neq 0$ states, and twice that for the $m_F=0$ state. Absorbing boundaries were used for the $m_F=0,-1,-2$ states.

The simulations reveal that all five Zeeman states are involved in determining the final form of the atom laser output. The $m_F=-2$ state has the least effect, as it is not strongly populated, and it quickly disperses in its antitrapping potential. However, the $m_F=-1$ antitrapped state is highly populated and is directly involved in the loss of the initial pulse for the case of Fig. 2(c). The simulation in the left section of Fig. 3 shows how the first $m_F=0$ atom laser pulse is destroyed by the second rf pulse: it transfers nearly all of the $m_F=0$ component, produced by the first pulse, into the other four Zeeman states (second row, Fig. 3). A new $m_F=0$ pulse, somewhat lower than the first, originates from the $m_F=-1$ state. However, it retains the momentum spread due to the antitrapping potential, which causes it to disperse and be lost, so that it is not observed in the experiment.

The second atom laser pulse is in fact two distinct pulses; an upper one originating from the $m_F=2$ state, and a lower one from the $m_F=1$ state. This can be seen most clearly in the third row of Fig. 3, after they have become well separated. Since the two pulse components are not resolvable in the experiment, this is an example of the dynamics revealed by simulation. These components have different initial momenta. The $m_F=1$ component, which originated from the $m_F=2$ state in the first rf pulse, was moving down towards its trap equilibrium when the second rf pulse arrived.

The lower $m_F=0$ pulse created by the second rf pulse escapes the fate of the first pulse because its downward momentum takes it lower than the first pulse, away from resonance. In fact, its position is close to that of the upper second $m_F=0$ pulse during the third rf pulse in the case of Fig. 2(b), and it survives for similar reasons. This can be seen by comparing the bottom rows of the $m_F=0$ columns of Fig. 3. Similarly the simulations explain the relative intensity of the first and second $m_F=0$ pulses in the experimental case of Fig. 2(b).

We have shown, for the case of the $F=2$ atom laser, that beyond a critical flux the classical fluctuations on the output beam increase with increasing flux. The fluctuations we have characterized are inherent to state changing out coupling. In future applications to precision measurement, these fluctuations must be either removed by feedback or avoided if the quantum noise limit of measurement is to be achieved. The prospect of combining atom lasers with atom chips opens up enormous possibilities in precision measurement. Considerations of the trade off between classical fluctuations and flux in atom lasers will be important in many applications in this field. We would expect many of the effects described here to be smaller for the $F=1$ atom laser but not absent. Rather than the two trapped states present in the $F=2$ laser, only the $m_F=-1$ state is trapped. Although atoms in the $m_F=1$ state are antitrapped for the $F=1$ laser, this state would be significantly populated for strong out coupling and could be expected to contribute to classical fluctuations on the $m_F=0$ output beam just as the antitrapped $m_F=-1$ state does for the $F=2$ laser studied in this paper.

The effects that we have described will be important not only for pulsed atom lasers, but also for unpumped continuous atom lasers. Just as in the pulsed case, at high flux, atoms

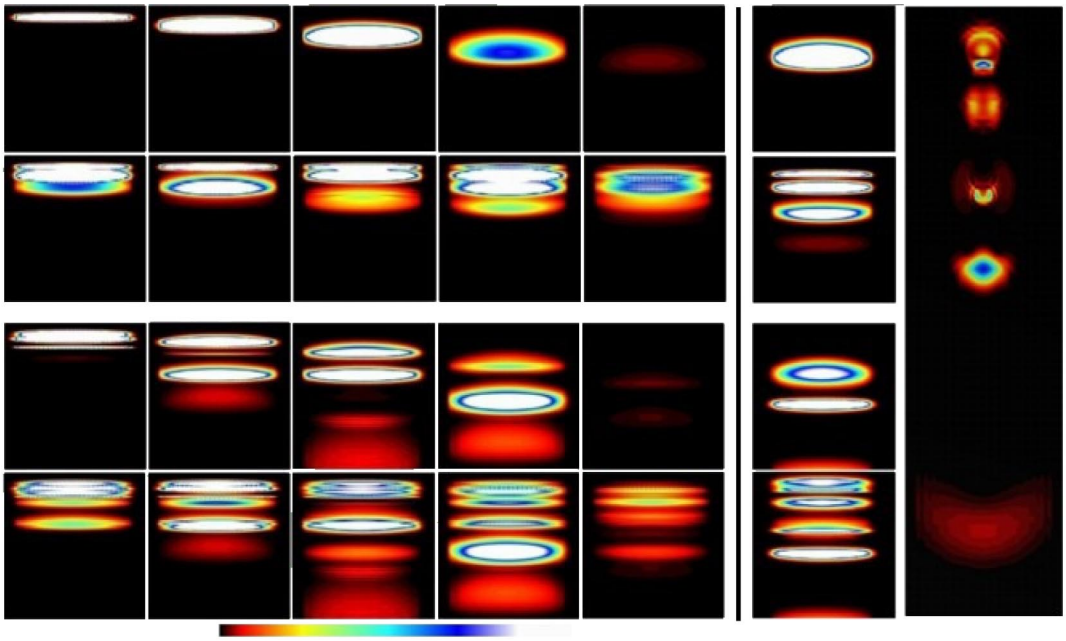

FIG. 3. (Color online) Numerical simulations of the cases of Figs. 2(c) and 2(b). Figure 2(c) is to the left of vertical line. Each image shows the GP wave function density, in arbitrary units, integrated through the tight trap direction. Density is indicated by the colobar at the bottom of the figure, with black and white corresponding to zero and high density, respectively. Each image is 120 μm in both directions. From top to bottom the rows are $t=1.2$ ms, just before the second rf pulse; just after the second rf pulse; $t=2.4$ ms, just before the third rf pulse; just after the third rf pulse. $t=0$ is the beginning of the first rf pulse. The columns from left to right are the $m_F=2,1,0,-1,-2$ states. The top-left image therefore shows the trapped position of the initial $m_F=2$ condensate. Figure 2(b) is to the right of vertical line. Only the $m_F=0$ state is shown. The rows are as before but the rf pulses occur at $t=1.6$ ms and $t=3.2$ ms. Each image is 120 μm vertically and 140 μm horizontally. The rightmost image shows the $m_F=0$ state density on a slice plane through the tight trap direction, just after the third rf pulse. It is 40 μm horizontally and about 150 μm vertically, allowing the first pulse to be seen. Simulation parameters: $\Delta=-633$, $\Omega=457$. See text for discussion.

will not only be coupled to the output beam, they will also be coupled to other trapped and untrapped Zeeman states and can be backcoupled from the output beam to the condensate. The situation is complex and requires detailed investigation. The quantitative comparison between theory and experiment presented here is important for the future development of atom laser sources for precision measurement. This is particularly true for the development of the pumped atom laser, one of the most important and sought-after devices in the field of atom optics.

This research was supported by the Australian Partnership for Advanced Computing and the Australian Research Council Centre of Excellence for Quantum Atom Optics.

[1] S. L. Rolston and W. D. Phillips, Nature (London) **416**, 219 (2002); W. Ketterle, Phys. Today **52**, 30 (1999).
[2] T. L. Gustavson *et al.*, Phys. Rev. Lett. **78**, 2046 (1997).
[3] See, for example, *Solid-state Laser Engineering* (Walter Koechner, Berlin, 1992), and references therein.
[4] S. A. Haine *et al.*, Phys. Rev. Lett. **88**, 170403 (2002).
[5] M.-O. Mewes *et al.*, Phys. Rev. Lett. **78**, 582 (1997).
[6] E. W. Hagley *et al.*, Science **283**, 1706 (1999).
[7] I. Bloch *et al.*, Phys. Rev. Lett. **82**, 3008 (1999).
[8] I. Bloch *et al.*, Phys. Rev. Lett. **87**, 030401 (2001).
[9] M. Köhl *et al.*, Phys. Rev. Lett. **87**, 160404 (2001).
[10] I. Bloch *et al.*, Nature (London) **403**, 166 (2000).
[11] B. P. Anderson and M. A. Kasevich, Science **282**, 1686 (1998).
[12] Y. Le Coq *et al.*, Phys. Rev. Lett. **87**, 170403 (2001).
[13] M. Köhl *et al.*, Phys. Rev. A **65**, 021606 (2002).
[14] R. J. Ballagh *et al.*, Phys. Rev. Lett. **78**, 1607 (1997).
[15] J. Schneider and A. Schenzle, Appl. Phys. B: Lasers Opt. **69**, 353 (1999).
[16] H. Steck *et al.*, Phys. Rev. Lett. **80**, 1 (1998).
[17] M. W. Jack *et al.*, Phys. Rev. A **59**, 2962 (1999).
[18] G. M. Moy *et al.*, Phys. Rev. A **59**, 667 (1999).
[19] G. Cennini *et al.*, Phys. Rev. Lett. **91**, 240408 (2003).
[20] T. Esslinger *et al.*, Phys. Rev. A **58**, R2664 (1998).
[21] R. Graham and D. F. Walls, Phys. Rev. A **60**, 1429 (1999).
[22] Australian Partnership for Advanced Computing National Facility: URL http://nf.apac.edu.au
[23] B. M. Caradoc-Davies, Ph.D. thesis, University of Otago, http://www.physics.otago.ac.nz/bec2/bmcd/